



A THEORETICAL ANALYSIS AND CFD SIMULATION ON THE CERAMIC MONOLITH HEAT EXCHANGER

Young Hwan Yoon¹, Jin Gi Paeng² and Ki Chul Kim³

ABSTRACT

A ceramic monolith heat exchanger is studied to find the performance of heat transfer and pressure drop by numerical computation and ξ -NTU method. The numerical computation was performed throughout the domain including fluid region in exhaust gas side rectangular ducts, ceramic core and fluid region in air side rectangular duct with the air and exhaust in cross flow direction. In addition, the heat exchanger was also analyzed to estimate the performance by conventional ξ -NTU method with several Nusselt number correlations from literature for flow in rectangular duct. By comparisons of both performances by the numerical computation and the ξ -NTU method, the effectiveness by ξ -NTU method was closest to the result by the numerical computation within the relative of 2.14% when Stephan's Nusselt number correlation was adopted to the ξ -NTU method among the several correlations.

Keywords: Ceramic Recuperator, Cross flow, Effectiveness, HRU, Conjugate heat transfer, Pressure drop

INTRODUCTION

Demand of world energy consumption is steadily growing due to development of industries and increase of population. However, fossil fuels most available at this time will be exhausted in near future. Moreover, the fossil fuels cause environmental pollution and global warming. Therefore, fuel cell systems become interested in energy market for alternative energy sources.

SOFC- solid oxide fuel cell of various fuel cell types has more than 60% of electric conversion efficiency, but produces high exhaust gas temperature of 600~1000°C. Therefore, a recuperator is need to recover the high temperature heat. Accordingly, heat resistance material is necessary for the high temperature heat exchanger. The recovered heat may be used to generate electricity utilizing a gas turbine as SOFC/GT hybrid power generating system as shown Fig. 1. Recently, a hybrid recuperator is interested for the power system. The hybrid recuperator consists of 3 pass recuperator, the first one is ceramic heat exchanger of which working temperature is from 600°C to 1,000°C, and the second and the third ones are metallic heat exchanger of which working temperature is under 600°C as shown in Fig. 2. For reference,

¹ Corresponding author: Department of Mechanical Engineering, Changwon National University, Changwon, Republic of Korea
e-mail: yhyoon@changwon.ac.kr

² School of Mechanical and Aerospace Engineering, Gyeongsang National University, Jinju, Gyeongnam, Republic of Korea

³ Department of Mechanical Engineering, Graduate School, Changwon National University

working temperatures of most conventional heat exchangers are generally less than 150°C.

In this study, the ceramic heat exchanger of 3 pass recuperator was analyzed to predict the performance, for example, heat transfer rate, effectiveness, and pressure drop, and so on since the ceramic heat exchanger has characteristics of cheap material cost, but low thermal efficiency compared to metallic heat exchangers.

Most research papers on heat exchanger deal with only one passage of hot or cold fluid flows for the heat transfer characteristics[1]. However, in this paper, the numerical computation was carried out through the whole region of the ceramic heat exchanger from the hot fluid, via ceramic core, to cold fluid for the performance. Furthermore, the heat transfer rate is also evaluated by theoretical method of ξ -NTU with various Nusselt number correlations for comparison to the numerical computation.

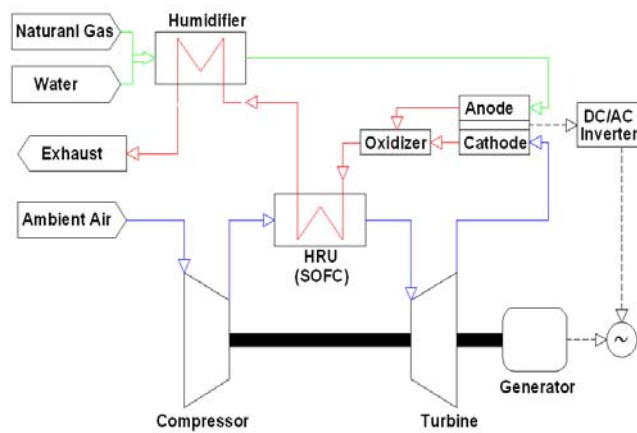


Fig. 1. Schematic of SOFC/GT hybrid power generating system

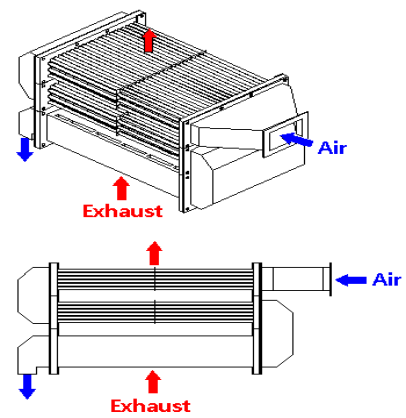


Fig. 2. Schematic drawing of SOFC/GT hybrid recuperator

THEORY

2.1 DESIGN AND ANALYSIS MODEL OF THE CERAMIC RECUPERATOR

The ceramic recuperator consists of rectangular hot exhaust and cold air passages with the exhaust and air in cross flow direction without mixing each other as shown in Fig. 3.

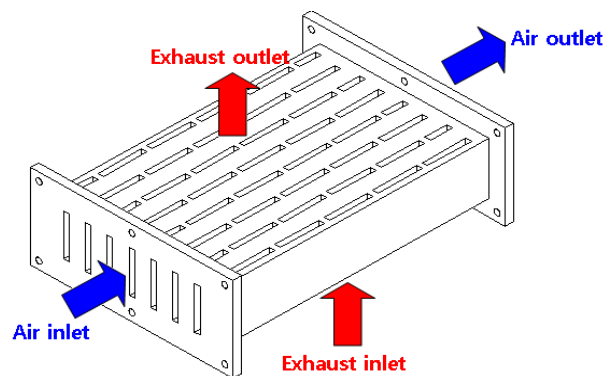


Fig. 3. Schematic drawing of the ceramic heat exchanger

2.2 OVERALL HEAT TRANSFER COEFFICIENT OF THE CERAMIC HEAT EXCHANGER

Overall heat transfer coefficient, U , between hot fluid and cold fluid is a principal factor for estimating the rate of heat transfer and expressed as Eq. (1).

$$U = \frac{1}{\frac{A}{A_{air} h_{air}} + \frac{\Delta X}{k} + \frac{A}{\eta_t A_{gas} h_{gas}}} \quad (1)$$

Here, k is thermal conductivity of the ceramic core, ΔX is the thickness of the wall, and A is the total heat transfer area. In addition, A_{air} and A_{gas} are air side and exhaust side heat transfer area, and h_{air} and h_{gas} are also each side average convective heat transfer coefficients, which are obtained from Nusselt relation of Eq. (2).

$$h = Nu \times \frac{k}{D_h} \quad (2)$$

k of above equation is thermal conductivity of each fluid and D_h is a hydraulic diameter of the rectangular fluid passage. Correlation equations of the Nusselt number from literature are listed in Table 1. The equations in Table 1 were derived under fully developed or developing flow conditions with constant wall heat transfer rate ($q_w'' = \text{const}$).

2.3 ξ -NTU METHOD

The thermal performance of the ceramic heat exchanger was calculated by theoretical equation of ξ -NTU method for which the effectiveness (ξ) is expressed as Eq. (3) in unmixed fluid flow condition, and then compared to that by the numerical computation.

$$\xi = 1 - \exp \left\{ \frac{NTU}{C} \left[\exp(-CNTU^{0.78}) - 1 \right] \right\} \quad (3)$$

Here, C is the ratio of heat capacity (C_{min}/C_{max}). NTU is defined by the total conductance (UA) divided by minimum heat capacity (C_{min}), where C_{min} is the lower heat capacity ($C_{min} = \dot{m} \times c_{p \min}$) and C_{max} is the higher heat capacity ($C_{max} = \dot{m} \times c_{p \max}$) of the two fluids with \dot{m} and c_p are mass flow rate and specific heat of the hot and cold fluids, respectively. Then, the rate of heat transfer from hot fluid to cold fluid can be computed as Eq. (4).

$$q = \xi \times C_{\min}(T_{gas_in} - T_{air_in}) \quad (4)$$

Outlet temperatures of exhaust and air (T_{air_out} and T_{gas_out}) are evaluated with inlet temperatures of both fluids as Eq. (5) and Eq. (6).

$$T_{air_out} = T_{air_in} + \frac{q}{c_{p_air}} \quad (5)$$

$$T_{gas_out} = T_{gas_in} + \frac{q}{c_{p_gas}} \quad (6)$$

2.4 PRESSURE DROP

Pressure drop is a major factor for the rating of the heat exchanger with the heat transfer rate. The Darcy friction equation is provided for the pressure drop in Eq. (7)[6].

$$\Delta P_{core} = f \frac{1}{2} \rho_m V_m^2 (L/D_h) \quad (7)$$

Here, $f = \frac{64}{Re}$

Table 1. Correlations of Nusselt number in a duct from the literature

Reference	Correlation	Condition		Range of validity
		Geometry	Flow regime	
Kay and Crawford[2]	$Nu_{fd} = 8.235(1 - 1.883/\alpha + 3.767/\alpha^2 - 5.814/\alpha^3 + 5.361/\alpha^4 - 2/\alpha^5)$	Rectangular	Fully developed	$Re < 2200$
Sieder-Tate[3]	$Nu = 1.86(RePrD/L)^{1/3} (\frac{\mu_f}{\mu_w})^{0.14}$	Circular	Simultaneously developing	$Re < 2200$
Stephan and preußer[4]	$Nu = 4.364 + \frac{0.086(RePrD/L)^{1.33}}{1 + 0.1Pr(ReD/L)^{0.83}}$	Circular	Simultaneously developing (constant wall heat flux)	$0.7 < Pr < 7$ or $RePrD/L < 33$ (for $Pr > 7$)
Shah and London[5]	$Nu = \begin{cases} 1.953(RePr\frac{D}{L})^{1/3} & (RePr\frac{D}{L}) \geq 33.3 \\ 4.364 + 0.0722RePr\frac{D}{L} & (RePr\frac{D}{L}) < 33.3 \end{cases}$	Circular	Thermally developing laminar (constant wall heat flux)	-

NUMERICAL ANALYSIS

There are seldom experimental data for the thermal performance of the present ceramic monolith heat exchanger in literature. Therefore, it is needed that the numerical computation of conjugate heat transfer

including fluid regions and ceramic solid region to find out the performance.

3.1 GOVERNING EQUATIONS

For the computations, the fluid flows were assumed to be 3-dimensional, incompressible, and steady state. All fluid flows of both cold fluid and hot exhaust were assumed to be laminar since the Reynolds number is less than 2,300. The governing equations for steady state and laminar flow are written as

Continuity equation

$$\frac{\partial}{\partial x_j}(\rho u_j) = 0 \quad (8)$$

Momentum equation

$$\frac{\partial}{\partial x_j}(\rho u_j u_i) = -\frac{\partial P}{\partial x_i} + \frac{\partial \tau_{ij}}{\partial x_j} \quad (9)$$

Here, P : Static pressure

τ_{ij} : Stress tensor

$$\tau_{ij} = \left[\mu \left(\frac{\partial u_i}{\partial x_j} + \frac{\partial u_j}{\partial x_i} \right) \right] - \frac{2}{3} \mu \frac{\partial u_k}{\partial x_k} \delta_{ij}$$

Energy equation

$$\rho c_p \frac{\partial}{\partial x_j}(u_j T) = k \frac{\partial^2 T}{\partial x_j^2} \quad (10)$$

3.2 COMPUTATIONAL GRID

Drawing of the ceramic heat exchanger is given in Fig. 4 with its dimension. The numerical analysis domain is the half of the whole heat exchanger as red line indicated in the figure since the heat exchanger is symmetric. Fig. 5 presents the computational grids determined by Gambit meshing. The total dimension of the numerical model is $305.5 * 497.5 * 65 \text{ mm}^3$ with about 800,000 cells made of hexahedron. FLUENT commercial software developed by finite volume method was used in this computation.

In order to check the sensitivity of the cell number, the number of cells was increased from 200,000 to 800,000 as Fig. 6. From the figure, there is less than 0.3% error in air side pressure drop with cell numbers of 700,000 to that with 800,000 by assuming that the solution with 800,000 cells were the exact solution. Therefore, the cell size was determined to be 800,000 for all numerical computations in this study.

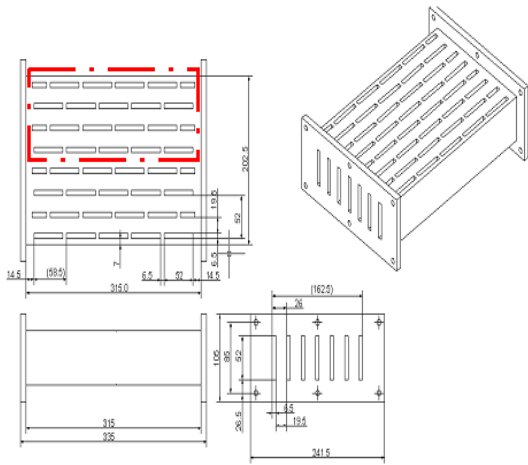


Fig. 4 Drawing of the ceramic exchanger core with its dimension

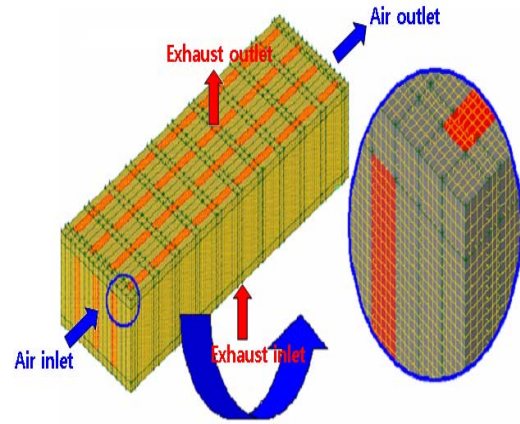


Fig. 5 Schematic drawing of the ceramic heat exchanger

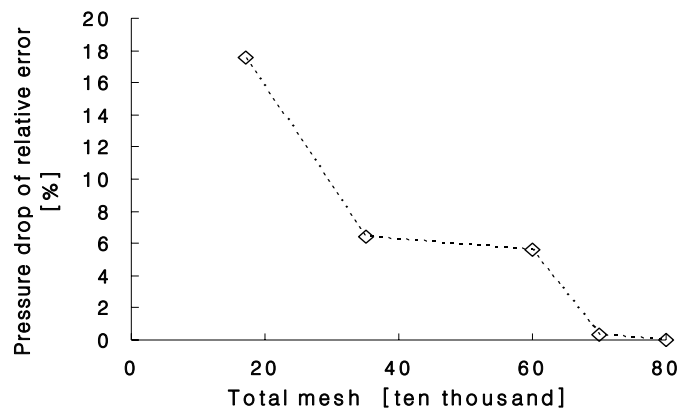


Fig. 6 Sensitivity of mesh grid

3.3 BOUNDARY CONDITIONS

3.3.1 Inlet boundary condition

Profiles of inlet velocity and temperature are needed for boundary conditions of cold air and hot exhaust. In this computation, uniform velocity profiles to the principal direction to the flow passage are assigned at the inlet according to the mass flow rate, but the two velocity components perpendicular to the principal directions were assumed to be zero. Temperature is also assumed to be uniform at inlet as Eq. (11).

$$T = T_{in} \quad (11)$$

3.3.2 Exit boundary condition

Atmospheric pressure is given to each exit for flow passages since the exit is open to atmosphere.

3.3.3 Wall boundary condition

Non-slip conditions were applied on walls of all fluid flows as Eq. (12). Adiabatic condition was imposed at outer walls of the ceramic core except walls of flow passages for cold air and hot exhaust as Eq. (13).

$$U_{wall} = V_{wall} = W_{wall} = 0 \quad (12)$$

$$\frac{\partial T}{\partial x_i} = 0 \quad (13)$$

COMPUTATIONAL RESULTS

Numerical computations of the heat transfer characteristics for the ceramic heat exchanger were compared to theoretical calculation of the heat transfer with various Nusselt number correlations from literature.

Before the computations, thermodynamic properties were tested by assuming in two ways such that one is constant properties at a average temperature of inlet and outlet temperatures and the other one is a linear function to the fluid temperature. For example, Table 2 presents us the air properties at 631 °C and the exhaust properties at 787 °C. Table 3 also gives the properties of ceramics core for the numerical computation.

Fig. 7 shows computations with the two assumptions for thermodynamic properties. In the figure, It is seen that the two computations(dotted and solid lines) are almost close to each other with the relative errors of 0.1 to 0.22%. Therefore, thermodynamic properties were assumed to be constant at an average fluid temperature later on.

The numerical computations were carried out at the exhaust mass flow rate of 0.001983 kg/s with varying the air flow rate from 0.001983 kg/s to 0.003966 kg/s at five steps. The Reynolds numbers according to the mass flow rates are written in Table 4.

For an instance, Fig. 8 presents contours of temperature distribution of the air flow at Reynolds number of 585 and the exhaust flow at Reynolds number of 79, which means that the mass flow rates of the air and the exhaust are the same at 0.001983 kg/s as shown in Table 5. The air flows, in (a) of Fig. 8, from left side to right side of the figure so that the air temperature is getting higher from the left inlet to the right exit. Contrarily, the exhaust gas flows, in (b) of Fig. 8, from bottom to upside so that the temperature is cooled from high inlet temperature to low exit temperature. Furthermore, Fig. 9 gives temperature profiles of the ceramic core at the same condition of Fig. 8. It can be also seen that the temperature is getting higher from left end to right end of the heat exchanger as the air temperature is increased from the left inlet to the right exit.

For the theoretical calculation of the heat transfer, the total heat transfer coefficient, U , between hot

exhaust and cold air should be evaluated with various Nusselt number correlations from literature as Eq. (1) and Table 1. Fig. 10 shows 4 lines of the total heat transfer coefficient related with Nusselt number correlations of Kays and Crawford[2], Sieder and Tate[3], Stephan[4], and Shah and London[5]. In the figure, the total heat transfer coefficient by of Kays and Crawford is highest and invariant to Reynolds number since the correlation is under fully developed flow condition, All except this line are increasing to Reynolds number since these are under developing flow condition.

Table 2. Fluid properties for CFD analysis ($Re_{Dh}=585$)

Properties	Air side	Exhaust side
	mean temperature 631[°C]	mean temperature 787[°C]
ρ [kg/m ³]	0.391	0.340
c_p [J/kgK]	1111.7	1138.7
k [W/mK]	0.062	0.070
μ [kg/ms]	3.875×10^{-5}	4.300×10^{-5}

Table 3. Thermodynamic properties of ceramic core ($Re_{Dh}=585$)

Properties	Ceramic core
ρ [kg/m ³]	3100
c_p [J/kgK]	670
k [w/mK]	77.5

Table 4. Mass flow rate according to the Reynolds number (Exhaust flow fixed)

Air side		Exhaust side	
Re_{Dh}	\dot{m}_{air} [kg/s]	Re_{Dh}	\dot{m}_{gas} [kg/s]
585	0.001983	79	0.001983
736	0.002479		
888	0.002975		
1040	0.003471		
1192	0.003966		

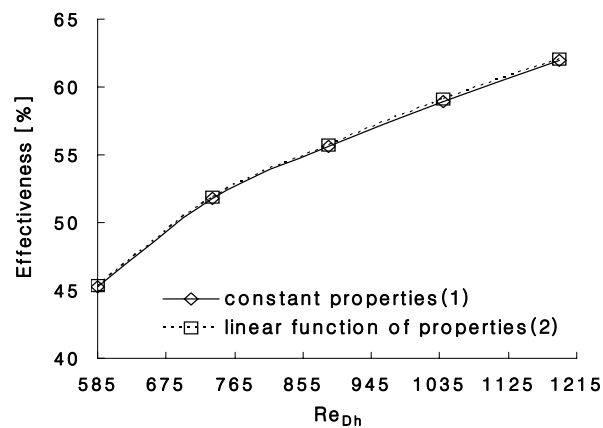


Fig. 7 Comparison between solutions with constant properties and linear function of the properties

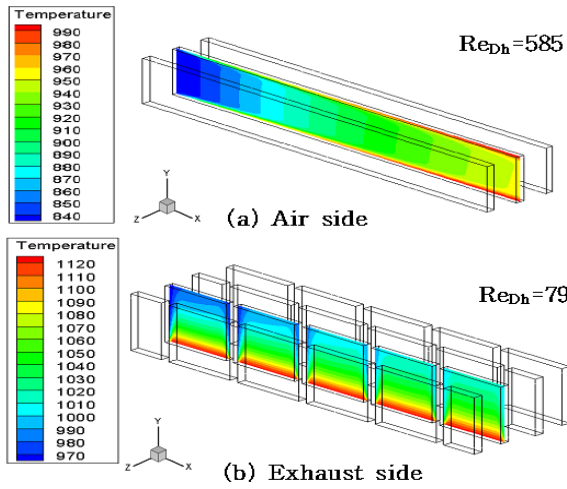


Fig. 8 Contours of temperature distributions of air and exhaust flows [unit : k]

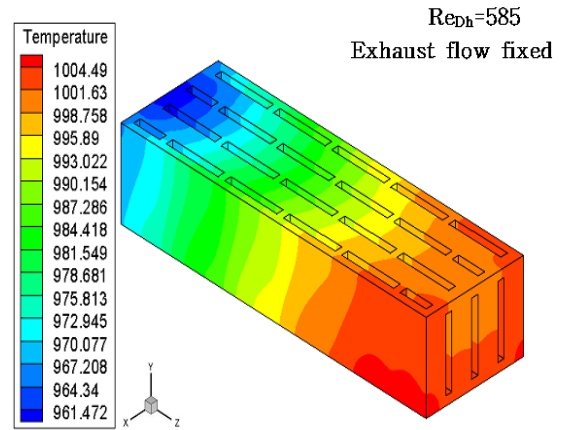


Fig. 9 Contours of temperature distributions of ceramic core [unit : K]

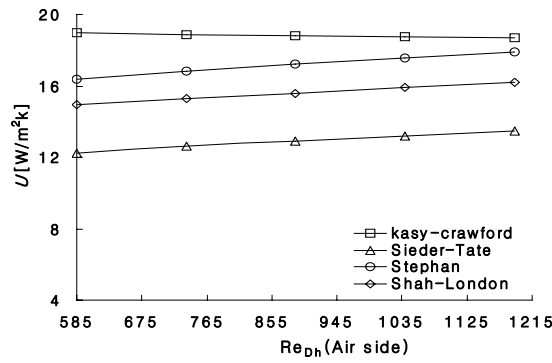


Fig. 10 Comparison of overall heat transfer coefficient with various correlations of Nusselt number

The effectiveness of a ceramic heat exchanger is defined as actual heat transfer rate over maximum possible heat transfer rate as Eq. (14)

$$\xi = \frac{C_h(T_{gas_in} - T_{gas_out})}{C_{min}(T_{gas_in} - T_{air_in})} = \frac{C_c(T_{air_out} - T_{air_in})}{C_{min}(T_{gas_in} - T_{air_in})} \quad (14)$$

Fig. 11 presents comparison between the effectiveness by the numerical computation (dotted line) and the effectiveness by the theoretical equation of Eq. (3) (solid line) with the various Nusselt number correlations. From the figure, the relative errors of the effectiveness are 2.8~7.2% for Kays and Crawford[2], 13.0 ~14.4% for Sieder and Tate[3], 0.25~2.14% for Stephan[4], and 3.5~4.6% for Shah and

London[5] to the effectiveness by the numerical computation, respectively. The largest error is up to 14.4% and the Stephan's correlation(circle marks) is closest to that by numerical computation(dotted line).

Total heat transfer rate of the ceramic heat exchanger is plotted in Fig. 12 by the same manner with Fig. 11. This figure shows us almost the same trend with the effectiveness of Fig. 11 since the total heat transfer rate is proportional to the effectiveness at a certain condition.

The exit temperature of each fluid is provided in Table. 5, which is obtained by the numerical computation and ξ -NTU method at the smallest Reynolds of 585 and largest Reynolds number of 1192 in this study, respectively. The relative error between the exit temperatures by the numerical computation and ξ -NTU method was less than 0.44% for the exhaust and less than 1.15% for the air.

Fig. 13 shows two lines of air side pressure drop which are a dotted line obtained by numerical computation and a solid line calculated with the head loss equation of Eq. (7). As shown in the figure, the pressure drop by the numerical computation is much higher up to 14~17% than that by the head loss equation. The reason may be deduced such that the fluid flow by the numerical computation is under developing flow condition from uniform inlet velocity profile, in the other hand, the head loss equation is only applicable to fully developed fluid flow condition which produces lower pressure drop relatively to developing flow. The difference of exhaust side pressure drop between them was up to 29% as Table. 6.

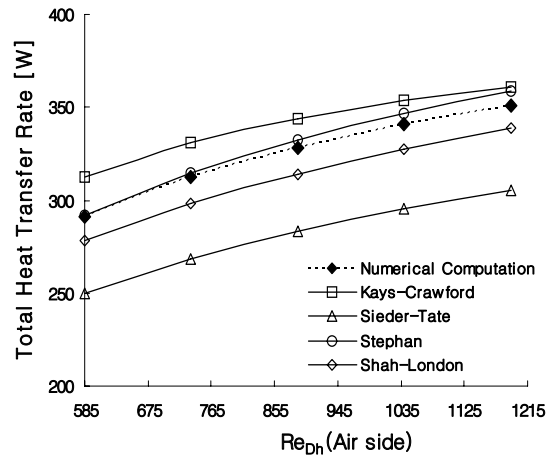
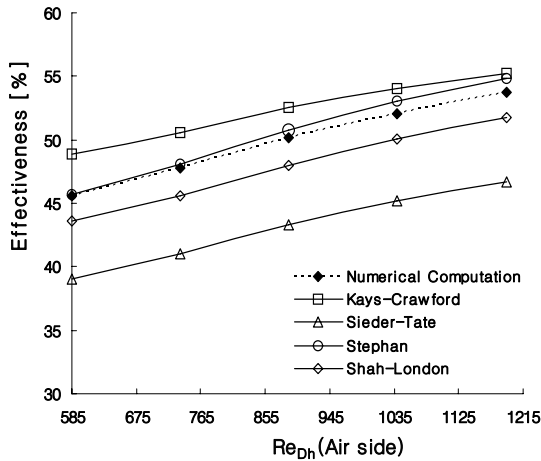


Fig. 11 Comparison of effectiveness between numerical computation and ξ -NTU method with various correlations of Nusselt number

Fig. 12 Comparison of total heat transfer from numerical computation and ξ -NTU method

Table 5. Comparison of outlet fluid temperatures between numerical computation and ξ -NTU method (Fixed exhaust flow rate)

Re_{D_h}	Air side temperature [°C]			Exhaust side temperature [°C]		
	Inlet	Outlet		Inlet	Outlet	
		Numerical computation	ξ -NTU		Numerical computation	ξ -NTU
585	560	700	693	850	722	721
1192	560	652	642	850	695	691

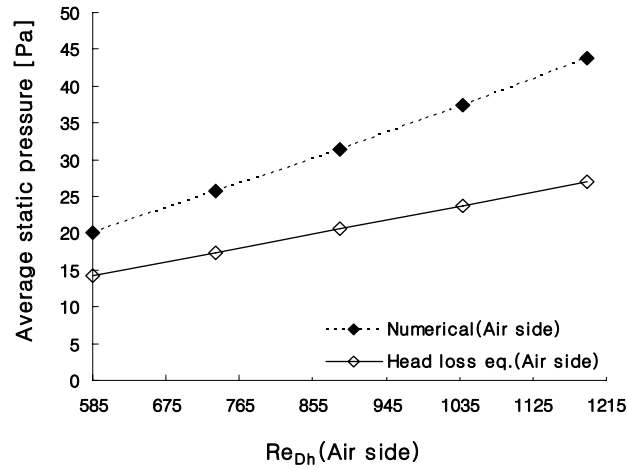


Fig. 13 Comparison of air side pressure drop from numerical computation and head loss equation according to Reynolds number

Table 6. Comparison of exhaust side pressure drop from numerical computation and head loss equation

Re _{Dh}	Exhaust side	
	Numerical computation[Pa]	Head loss equation[Pa]
24	0.78	0.56

CONCLUSIONS

In this study, The numerical computations were carried out through hot exhaust, ceramic core, and cold air in the whole region of the ceramic heat exchanger for 800~1,000°C. The effectiveness and the total heat transfer rate by the numerical computation were compared with those by ξ -NTU method using various Nusselt number correlations from literature

(1) The relative errors of the total heat transfer by ξ -NTU method using five Nusselt number correlations from literature were less than 14.4% to that by the numerical computation. Among the Nusselt number correlations, The total heat transfer by ξ -NTU method with Stephan's correlation is closest to that by numerical computation.

(2) Accordingly, the exit temperature by ξ -NTU method with Stephan's correlation simulates within 1.15% of the relative error for exhaust exit temperature and 0.44% for the air exit temperature compared to the numerical computation.

(3) Pressure drops by the numerical computation were 14~17% higher than that by the head loss equation for air side flow passage and 29% higher for exhaust side flow passage since all fluid flows in passages of the ceramic heat exchanger are developing fluid flows which the present numerical computation simulated, in the other hand, the head loss equation is only applicable in fully developed condition which produces relatively lower pressure drop to the developing flow.

ACKNOWLEDGMENTS

This work is financially supported by the Ministry of Education and Human Resources Development(MOE), the Ministry of Commerce, Industry and Energy(MOCIE) and the Ministry of Labor(MOLAB) through the fostering project of the Industrial-Academic Cooperation Centered University. And this work was supported by the second phase Bk21 Project.

REFERENCES

- [1] Yun, J. W. and J. Y. Yun, (1995), Numerical study on the characteristics of flow and heat transfer in finned tube heat exchanger, Journal of SAREK, pp. 74-79.
- [2] Kays, W. M. and M. E. Crawford (1980), Convective heat and mass transfer, McGraw Hill, New York.
- [3] Incropera, F. P. and D. P. Dewitt (1996), Fundamentals of heat and mass transfer, John Wiley and Sons, New York.
- [4] Stephan, K. and P. Preußer (1979), Wärmeübergang und maximale Wärmestromdichte beim behältersieden binärer und ternärer flüssigkeitsgemische, Chem. Ing. 51 p. 37.
- [5] Shah, R. K. and A. L. London (1978), Laminar flow forced convection in duct, Supply 1, Adv. Heat transfer.
- [6] Mill. A. F. (2003), Basic Heat and Mass transfer, 2nd ed Prentice Hall, New Jersey, pp. 687-689.